

Synthesis, Aggregation, and Binding Behavior of Synthetic Amphiphilic Receptors

Albertus P. H. J. Schenning,[†] Beatriu Escuder,[†] Johanna L. M. van Nunen,[†] Bas de Bruin,[†] Dennis W. P. M. Löwik,[†] Alan E. Rowan,[†] Sjerry J. van der Gaast,[‡] Martinus C. Feiters,[†] and Roeland J. M. Nolte^{*,†}

Department of Organic Chemistry, NSR Center, University of Nijmegen, Toernooiveld, 6525 ED Nijmegen, The Netherlands, and The Netherlands Institute for Sea Research (NIOZ), P.O. Box 59, 1790 AB Den Burg Texel, The Netherlands

nolte@sci.kun.nl

Received May 22, 2000

Amphiphilic bowl-shaped receptor molecules have been synthesized starting from diphenylglycoluril. Upon dispersion in water, these molecules self-assemble to form vesicles that bind neutral guests and alkali metal ions. In the case of bis(alkylester)-modified receptor compound **4**, electron microscopy reveals that an increase in the size of the alkali metal ion (from Na⁺ or K⁺ to Rb⁺ and to Cs⁺) leads to a change in the shape of the aggregates, viz. from vesicles to tubules. Monolayer experiments suggest that this behavior is due to a change in the conformation of this amphiphilic receptor. In water, molecules of **4** have an elongated conformation that changes to a sandwich-like one upon binding of alkali metal ions. Binding studies with vesicles from the bis-ammonium receptors **6** and **9** and the guest 4-(4-nitrophenylazo)resorcinol (Mageson) reveal that below the critical aggregation concentration (CAC) of the amphiphile 1:1 host–guest complexes are formed with high host–guest association constants. Above the CAC, a host–guest ratio of 2:1 was observed that indicates that only the cavities on the outside of the vesicle can be occupied. In the case of the naphthalene walled compound **8** changes in the vesicle structure are induced by the organic guest Mageson.

Introduction

Receptors on cell membranes play a key role in substrate recognition and signal response in biological processes. For example, proteins and peptides can enter cells by first binding to specific surface receptors followed by rapid internalization.¹ This process, called receptor-mediated endocytosis, plays a fundamental role in the growth, nutrition, and differentiation of animal cells. Hemocyanins, the oxygen transport proteins from molluscs and arthropods, form aggregates upon binding alkali metals after which oxygen uptake can take place.² Binding to receptor sites is also an important step in the working mechanism of drugs. For instance, the antitumor compound paclitaxel decreases the growth of cancer cells by binding to the microtubuli.³

Artificial cell-surface receptors can give information on how membranes recognize extracellular signals and respond to them. This is a field of intense research with great potential application in diverse areas of chemistry, medicine, and biology such as catalysis, drug delivery, medical imaging, separation technology, and biomolecular sensing among others.⁴ Currently, most studies focus on molecular recognition processes in monolayers at the air–water interface,⁵ but only a few are dealing with interactions at vesicle surfaces.⁶

Aggregation of receptor molecules, e.g., aza-crown ether derivatives and cryptand-based amphiphiles, in water has been described in the literature.⁷ Several calixarenes bearing long aliphatic chains have been shown to form vesicles or micelles that can bind aromatic guest mol-

(4) (a) Lahiri, J.; Fate, G. D.; Ungashe, S. B.; Groves, J. T. *J. Am. Chem. Soc.* **1996**, *118*, 2347–2358. (b) Kikuchi, J.; Ariga, K.; Ikeda, K. *Chem. Commun.* **1999**, 547–548. (c) Schell, C.; Hombrecher, H. K. *Chem. Eur. J.* **1999**, *5*, 587–598. (d) Morita, T.; Kimura, S.; Imanishi, Y. *J. Am. Chem. Soc.* **1999**, *121*, 581–586.

(5) (a) Blankenburg, R.; Meller, P.; Ringsdorf, H.; Salesse, C. *Biochemistry* **1989**, *28*, 8214–8221. (b) Kurihara, K.; Ohto, K.; Tanaka, Y.; Aoyama, Y.; Kunitake, T. *J. Am. Chem. Soc.* **1991**, *113*, 444–450. (c) Kurihara, K.; Ohto, K.; Honda, Y.; Kunitake, T. *J. Am. Chem. Soc.* **1991**, *113*, 5077–5079. (d) Ikeura, Y.; Kurihara, K.; Kunitake, T. *J. Am. Chem. Soc.* **1991**, *113*, 7342–7350. (e) Pathiranan, S.; Neely, W. C.; Myers, L. J.; Vodyanoy, V. *J. Am. Chem. Soc.* **1992**, *114*, 1404–1405. (f) Qian, P.; Matsuda, M.; Miyashita, T. *J. Am. Chem. Soc.* **1993**, *115*, 5624–5628. (g) Heiney, P. A.; Gidalevitz, D.; Maliszewskyj, N. C.; Satija, S.; Vaknin, D.; Pan, Y.; Ford, W. T. *Chem. Commun.* **1998**, 1483–1484. (h) Gidalevitz, D.; Mindyuk, O. Y.; Stetzer, M. R.; Heiney, P. A.; Kurnaz, M. L.; Schwartz, D. K.; Ocko, B. M.; McCauley, J. P. Jr.; Smith, A. B. *J. Phys. Chem. B* **1998**, *102*, 6688–6691.

(6) (a) Carmona-Ribeiro, A. M. *Chem. Soc. Rev.* **1992**, 209–214. (b) Menger, F. M.; Angelova, M. I. *Acc. Chem. Res.* **1998**, *31*, 789–797 and references therein. (c) Bhattacharya, S.; Subramanian, M. *J. Org. Chem.* **1998**, *63*, 7640–7651. (d) Menger, F. M.; Nelson, K. H.; Guo, Y. *Chem. Commun.* **1998**, 2001–2002. (e) Klein Gebbink, R. J. M.; Sandee, A. J.; Peters, F. G. A.; van der Gaast, S. J.; Feiters, M. C.; Nolte, R. J. M. *J. Chem. Soc., Perkin Trans.* submitted.

(7) (a) Monserrat, K.; Grätzel, M.; Tundo, P. *J. Am. Chem. Soc.* **1980**, *102*, 5527–5529. (b) Gokel, G. W. *J. Chem. Soc., Chem. Commun.* **1992**, 520–522. (c) Munoz, S.; Mallen, J.; Nakano, A.; Chen, Z.; Gay, I.; Echegoyen, L. E. *J. Am. Chem. Soc.* **1993**, *115*, 1705–1711. (d) Tai, Z.; Qian, X.; Wu, L.; Zhu, C. *J. Chem. Soc., Chem. Commun.* **1994**, 1965–1966. (e) Behm, C. A.; Creaser, I. I.; Korybut-Daszkiewicz, B.; Geue, R. J.; Sargenson, A. M.; Walker, G. W. *J. Chem. Soc., Chem. Commun.* **1993**, 1844–1846. (f) Fyles, T. M.; Zeng, B. *J. Org. Chem.* **1998**, *63*, 8337–8345. (g) Ghosh, P.; Khan, T. P.; Bharadwaj, P. K. *Chem. Commun.* **1996**, 189–190. (h) Bandyopadhyay, P.; Bharadwaj, P. K. *Langmuir* **1998**, *14*, 7537–7538.

[†] University of Nijmegen.

[‡] The Netherlands Institute for Sea Research.

(1) Goldstein, J. L.; Anderson, R. G. W.; Brown, M. S. *Nature* **1979**, *279*, 679–685.

(2) Magnus, K. A.; Ton-That, H.; Carpenter, J. E. *Chem. Rev.* **1994**, *94*, 727–735.

(3) Nogales, E.; Grayer Wolf, S.; Khan, I. A.; Ludueña, R. F.; Downing, K. H. *Nature* **1995**, *375*, 424–427.

ecules.⁸ Murakami and co-workers have reported on amphiphilic octopus-type cyclophane receptors that form multiwalled vesicles in water.⁹ The cavities of these receptors are able to bind negatively charged aromatic guest molecules with high binding constants by an induced fit mechanism. More recently, steroid based amphiphiles bearing different headgroups have been incorporated into synthetic membranes.^{4b} Amphiphilic cyclodextrin diesters have also been reported to form micelles and vesicles in water; however, no binding studies were performed.¹⁰

We have previously shown that clip-shaped host molecules of type **1** (Figure 1A) are able to bind uncharged aromatic guest molecules, e.g., resorcinol, by π - π stacking and hydrogen bonding interactions.¹¹ Basket-shaped derivatives of **1** containing crown ether moieties in addition are capable of binding alkali metal ions and positively charged aromatic guests such as 1,1,4,4-dimethyl bipyridine (Figure 1B).¹² These properties have prompted us to synthesize amphiphilic derivatives of these host molecules by functionalizing **1** with crown ether moieties and long aliphatic chains and to investigate the self-assembling and binding features of this type of bowl-shaped surfactant molecules.

Compounds are shown in Scheme 1. We have prepared five new receptor surfactants (**4–6** and **8, 9**) from clips possessing different aromatic walls (benzene or naphthalene) and a variety of different headgroups (alkanoyloxyalkylamino, alkylamino, and alkylammonium groups). These amphiphiles form various types of aggregates upon dispersal in water and are able to bind alkali metals and uncharged aromatic guest molecules which modifies their supramolecular structure.^{13,14}

Results and Discussion

Synthesis. The amphiphilic bowl-shaped receptors **4–6** and **8, 9** were prepared as shown in Scheme 1. Compound **3** was synthesized under Finkelstein condition¹⁵ from **2** by a ring-closure reaction using 3-amino-

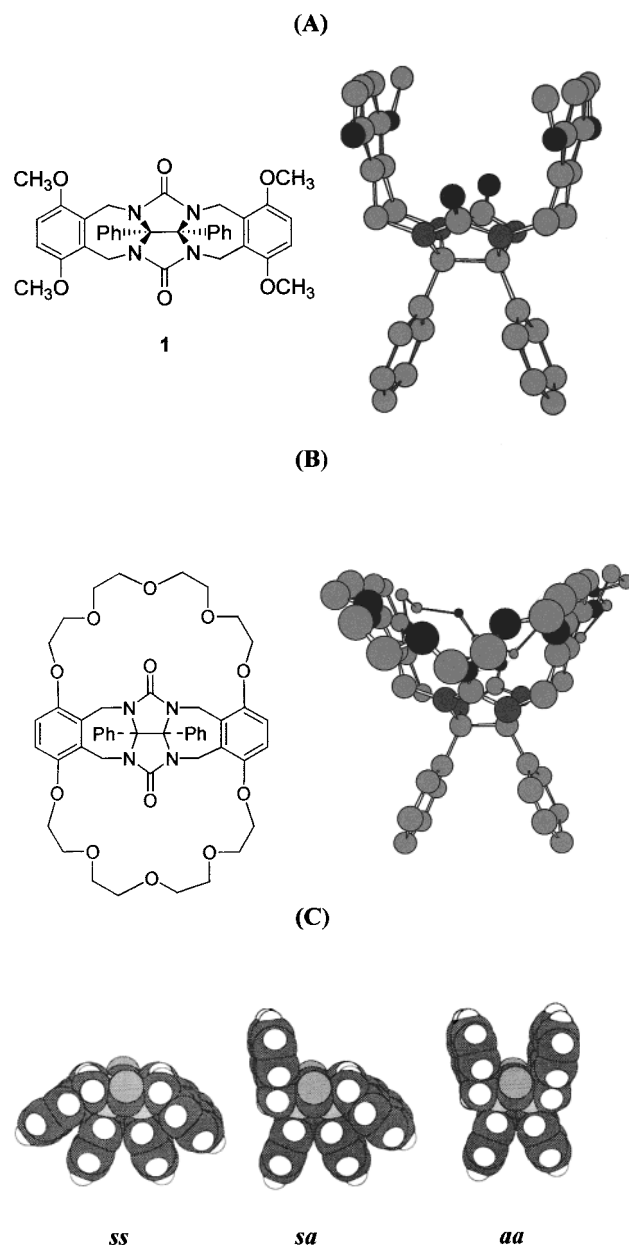


Figure 1. Molecular and X-ray structure of (A) a clip molecule **1** and (B) a polyoxabasket derivative of **1**. (C) Schematic representation of the three possible conformations of naphthalene walled clip and basket molecules.

propanol. Amphiphile **4** was obtained by esterification of **3** with undecanoic acid chloride. Compounds **5** and **8** were synthesized from **2** and **7**, respectively, by reaction with hexadecylamine under the same conditions as described above for **3**. The positively charged amphiphilic receptors **6** and **9** were obtained by subsequent methylation of compounds **5** and **8** with methyl tosylate in toluene.

Conformational Behavior. Host molecules based on diphenylglycoluril containing 1,8-connected naphthalene side walls (**7–9**) can exist in solution as a mixture of three conformers (*ss*, *sa*, and *aa*, Figure 1C), which interconvert slowly on the NMR time scale.^{16,17} Earlier work in our group has shown that these receptors bind guest mol-

(8) (a) Shinkai, S.; Mori, S.; Koreishi, H.; Tsubaki, T.; Manabe, O. *J. Am. Chem. Soc.* **1986**, *108*, 2409–2416. (b) Arimori, S.; Nagasaki, T.; Shinkai, S. *J. Chem. Soc., Perkin Trans. 2* **1995**, 679–683. (c) Tanaka, Y.; Miyachi, M.; Kobuke, Y. *Angew. Chem., Int. Ed.* **1999**, *38*, 504–506.

(9) (a) Murakami, Y.; Kikuchi, J.; Ohno, T.; Hayashida, O.; Kojima, M. *J. Am. Chem. Soc.* **1990**, *112*, 7672–7681. (b) Kikuchi, J.; Inada, M.; Murakami, Y.; Egami, K.; Suehiro, K. *J. Phys. Org. Chem.* **1997**, *10*, 351–357.

(10) Zhang, P.; Parrot-Lopez, H.; Tchoreloff, P.; Baskin, A.; Ling, C. C.; De Rango, C.; Coleman, A. W. *J. Phys. Org. Chem.* **1992**, *5*, 518–528.

(11) (a) Sijbesma, R. P.; Nolte, R. J. M. *J. Org. Chem.* **1991**, *56*, 3122–3124. (b) Sijbesma, R. P.; Kentgens, A. P. M.; Lutz, E. T. G.; van der Maas, J. H.; Nolte, R. J. M., *J. Am. Chem. Soc.* **1993**, *115*, 8999–9005. (c) Reek, J. N. H.; Priem, A. H.; Engelkamp, H.; Rowan, A. E.; Elemans, J. A. A. W.; Nolte, R. J. M., *J. Am. Chem. Soc.* **1997**, *119*, 9956–9964.

(12) (a) Smeets, J. W. H.; van Dalen, L.; Kaats-Richter, V. E. M.; Nolte, R. J. M. *J. Org. Chem.* **1990**, *55*, 454–461. (b) Schenning, A. P. H. J.; de Bruin, B.; Rowan, A. E.; Kooijman, H.; Spek, A. L.; Nolte, R. J. M. *Angew. Chem., Int. Ed. Engl.* **1995**, *34*, 2132–2133.

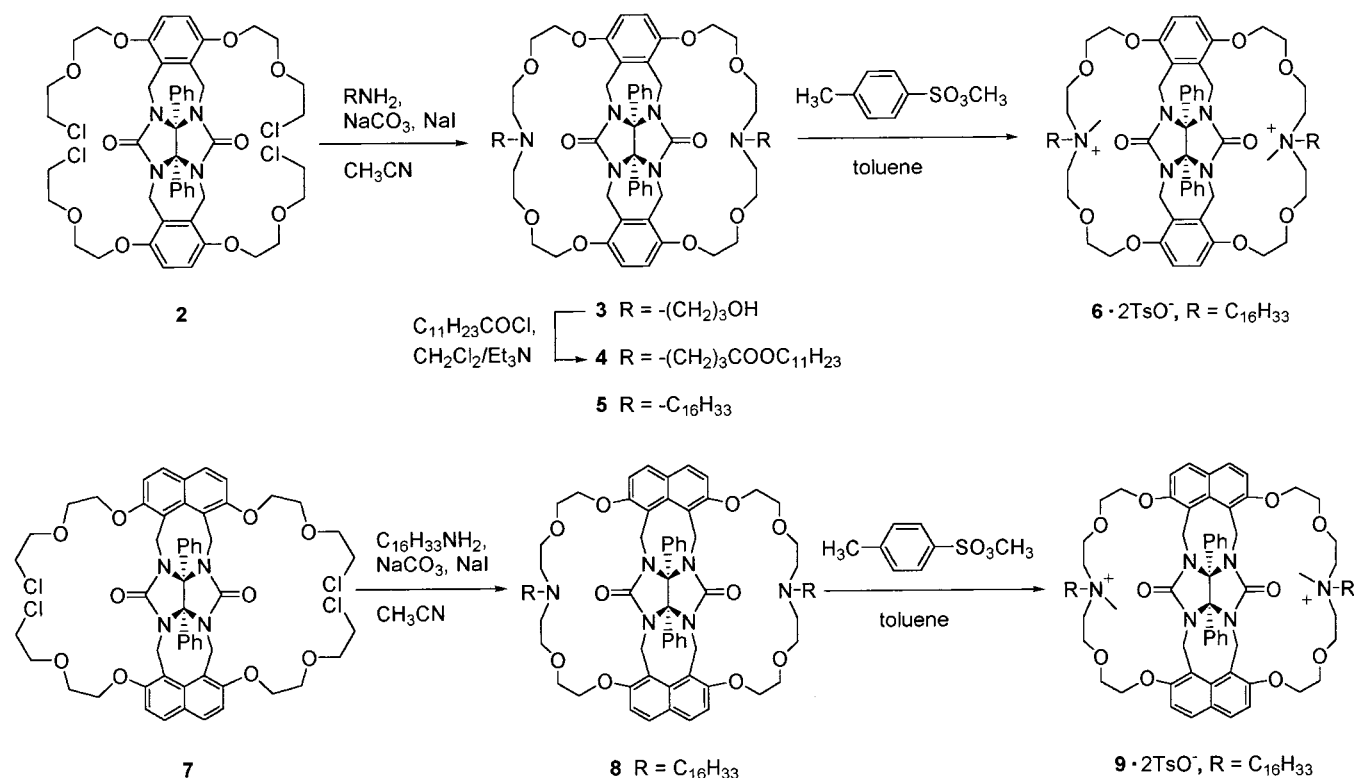
(13) Part of this work has been published as preliminary communications: (a) Schenning, A. P. H. J.; de Bruin, B.; Feiters, M. C.; Nolte, R. J. M. *Angew. Chem., Int. Ed. Engl.* **1994**, *33*, 1662–1663. (b) van Nunen, J. L. M.; Stevens, R. S. A.; Picken, S. J.; Nolte, R. J. M. *J. Am. Chem. Soc.* **1994**, *116*, 8825–8826.

(14) For other examples of artificial receptors based on bilayer membranes and their metal ion-induced morphological changes see: (a) Shinkai, S.; Nakamura, S.; Manabe, O.; Yamada, T.; Nakashima, N.; Kunitake, T. *Chem. Lett.* **1986**, 49–52. (b) Nakashima, N.; Moriguchi, I.; Nakano, K.; Takagi, M. *J. Chem. Soc., Chem. Commun.* **1987**, 617–619. (c) Kunitake, T.; Kim, J.-M.; Ishikawa, Y. *J. Chem. Soc., Perkin Trans. 2* **1991**, 885–890. (d) Singh, A.; Tsao, L.-I.; Markowitz, M.; Gaber, B. P. *Langmuir* **1992**, *8*, 1570–1577.

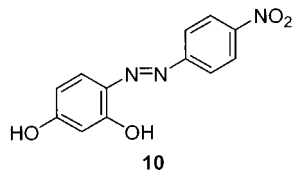
(15) Houben-Weyl. *Methoden der Organische Chemie*, Vol V/4; Georg Thieme: Stuttgart, 1952; p 595.

(16) Sijbesma, R. P.; Nolte, R. J. M. *J. Am. Chem. Soc.* **1991**, *113*, 6695–6696.

Scheme 1



ecules only in their *aa* conformation by an induced fit mechanism.¹⁶ Since knowledge of the conformational behavior of the receptors is important for our binding studies we performed ¹H NMR experiments on **8** and **9**. The most characteristic resonances of **8** and **9** are listed in Table 1. By comparison with ¹H NMR data of related compounds synthesized in our group¹¹ and by using Johnson–Bovey tables¹⁸ for ring current contributions, we were able to prove that in chloroform 90% of the molecules of amphiphile **8** exist in the *sa* conformation and 10% in the *ss* conformation, a ratio typical for this kind of bowl-shaped compounds.¹⁶ After addition of an excess of potassium thiocyanate, all molecules of **8** were found to be converted to the *aa* conformation, which is in agreement with earlier findings in our group on other clip molecules.¹⁶ The effect of the addition of aromatic guest molecules on the conformation of **8** was also investigated by NMR. Upon addition of 1 equiv of Magneson (4-(4-nitrophenylazo)resorcinol, compound **10**) to a 10 mM solution of **8** in CDCl₃ a small change in the ratio of conformers (*sa* conformer 85%, *ss* conformer 10%, *aa* conformer 5%) was observed.



Amphiphilic receptor **9** displayed the following distribution of conformers in chloroform: *sa* ~60%, *ss* ~15%, and *aa* ~25%. In this solvent the NMR resonances for

Table 1. ¹H NMR Signals (ppm) of the *ss*, *sa*, and *aa* Conformers of **8** and **9**^a

compd	NCH ₂ Ar syn	NCH ₂ Ar anti	naphth-H syn	naphth-H anti
8 sa	4.8, 6.0	4.1, 6.1	7.2, 6.8	7.75, 7.3
8 ss	5.1, 6.3		7.3, 6.8	
9 sa	4.8	6.1, 4.1	7.2	7.8, 7.26
9 ss	5.1		7.3	
9 aa		5.8		7.3

^a The ¹H NMR spectra of **8** were recorded with a 200 MHz NMR instrument in CDCl₃ and those of **9** with a 400 MHz instrument in CD₃OD. T = 25 °C.

receptor **9** were significantly broadened. This broadening can be attributed to aggregation and also to the fact that this molecule can exist as nine stereoisomers.¹⁹ In methanol, the ratios were slightly altered as follows: *sa* ~50%, *ss* ~20%, and *aa* ~30%. Addition of D₂O (MeOD/D₂O = 5/1, v/v) or doubling the concentration had a negligible effect (less than 5%) on the distribution of conformations of **9**.

Complexation Studies in Chloroform. We have previously shown that molecular clips such as **1** can bind aromatic substrates, e.g., resorcinol in chloroform.¹¹ Binding occurs by π – π stacking interactions between the two aromatic walls of the cavity of **1** and the aromatic ring of the guest and by hydrogen bonding of the phenolic OH groups of the guest with the urea carbonyl groups of the host as determined by IR and ¹H NMR spectroscopy. The chromophore-containing resorcinol derivative Magneson was chosen as a guest, in the present study, because its binding affinities toward host molecules can not only be measured by ¹H NMR but also by UV–vis

(17) Reek, J. N. H.; Engelkamp, H.; Rowan, A. E.; Elemans, J. A. W.; Nolte, R. J. M. *Chem. Eur. J.* **1998**, 4, 716–722.

(18) Johnson, C. S. Jr; Bovey, F. A. *J. Chem. Phys.* **1958**, 29, 1012–1015.

(19) In principle, each N⁺-methyl can exist in two configurations with the methyl substituent pointing in or out of the cavity. In combination with the conformational isomerization of the walls, this results in nine possible stereoisomers. These stereoisomers cannot be resolved by NMR.

Table 2. Association Constants and Binding Free Energies (ΔG s) of Complexes between Magneson (10) and Different Hosts in Chloroform at 25 °C

host	$\epsilon G - \epsilon HG (\times 10^3)^a$	$K_a (M^{-1})$	$-\Delta G (kJ/mol)$
1	9.7	720	16.3
1		690 ^b	16.2
5	18.7	2500	19.4
6	10.4	2200	19.0
8	27.0	850	16.7
9	17.0	1600	18.2

^a This value is the difference in extinction coefficient between the host–guest complex and the guest ($M^{-1}cm^{-1}$) at 438 nm. ^b This association constant was determined by ¹H NMR titration experiments.

Table 3. Complexation-Induced Shift (CIS) Values of Guests in Their Complexes with Hosts 1 and 6^a

guest	host	$\Delta\delta H^2 (ppm)$	$\Delta\delta H^4 (ppm)$	$\Delta\delta H^5 (ppm)$
Magneson	1	−1.71	−0.42	
resorcinol ^b	1	−2.71	−0.46	−0.30
resorcinol	6^c	−1.24	−0.25	−0.27

^a Solvent CDCl₃, $T = 25\text{ °C}$. ^b Data taken from ref 10. ^c FT-IR measurements showed that after complexation of resorcinol to **6** a 23 cm^{-1} shift of the carbonyl stretching vibration to lower wavenumber occurred.

titration experiments. This is an advantage because NMR measurements in water on aggregated host molecules are hampered by broadening of the resonances which makes accurate binding studies impossible. The titration experiments were carried out on compounds **1**, **5**, **6**, **8** and **9** initially in chloroform as the solvent. The binding constants were determined by UV–vis and ¹H NMR spectroscopy. The guest molecules resorcinol and Magneson were bound as 1:1 inclusion complexes. The association constants found are listed in Table 2. The complexation-induced shifts calculated from the NMR titration experiments are shown in Table 3.

The binding studies in chloroform (Table 2) show that Magneson indeed is bound to clip molecule **1**. The association constant of 720 M^{-1} determined by UV–vis spectroscopy agrees within experimental error (10%) with that calculated from ¹H NMR data ($K_a = 690\text{ }M^{-1}$). The complexation induced shifts determined from the ¹H NMR data (Table 3) indicate that Magneson is bound in the cleft of receptor **1**. This compound is a better receptor for resorcinol ($K_a = 2600\text{ }M^{-1}$) than for Magneson ($K_a = 690\text{ }M^{-1}$). This difference can be attributed to an intramolecular hydrogen bridge, which is known to exist between the OH group and one of the azo nitrogen atoms of Magneson.²⁰ For the bowl-shaped amphiphile **6** the same order of binding strength was observed for Magneson ($K_a = 2200\text{ }M^{-1}$) as for resorcinol ($K_a = 3400\text{ }M^{-1}$). The binding affinities of **5** and **6** for Magneson are almost the same (Table 2). In the case of **5** the nitrogen atoms in the crown ether rings can be involved in hydrogen bonding with the OH groups of Magneson.¹¹ Additional stabilizing interactions can exist between the quaternary ammonium groups of the **6** and the azo- π system of this guest.²¹ The binding constants of the complexes of Magneson with compounds **8** and **9** are lower than those of the complexes with **5** and **6**. This difference can be explained as being a result of the conformational behavior of **8** and **9** described in the previous section. Thus, the required change to the binding conformation costs free

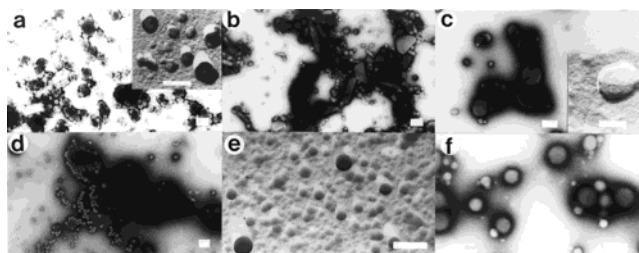


Figure 2. Transmission electron micrographs of dispersions in water of (a) amphiphile **4** (negative staining, inset freeze fracturing), (b) amphiphile **5** (negative staining), (c) amphiphile **6** (negative staining, inset freeze fracturing), (d) amphiphile **8** (negative staining), (e) amphiphile **8** (Pt-shadowing), and (f) amphiphile **9** (negative staining). Bars represent 200 nm.

energy which will lower the association constant. The free energy difference between the *aa* and *sa* conformations can be calculated from the ratio of these conformations in solution and is $\Delta G > 7.7\text{ kJ/mol}$ for compound **8** in chloroform and $\Delta G = 3\text{ kJ/mol}$ for compound **9** in methanol.¹⁹ The conformational change that occurs upon binding can be considered to be analogous to the induced fit mechanism in enzyme catalysis.²²

Aggregation Behavior in Water. Dispersion of the amphiphilic receptors **4–6** and **8**, **9** in water led to the formation of aggregates as could be deduced from electron microscopy (Figure 2). Compound **4** formed vesicles with diameters of 100–250 nm in deionized water (pH \approx 6) (Figure 2a). Amphiphile **5** formed vesicles and more extended structures (Figure 2b). Compound **8** yielded vesicle structures with diameters in the range of 50–250 nm (Figure 2d,e). Receptor molecules **6** and **9** also gave vesicles with diameters of 100–500 nm and 50–200 nm, respectively (Figure 2c,f).

The vesicles formed by bowl-shaped amphiphiles **6** and **9** were characterized further to obtain information about the molecular architectures of this type of aggregates. The particle size distribution of aggregate solutions of **6** as determined by light scattering (Figure 3A)²³ revealed the existence of two types of spherical aggregates: one with a diameter of approximately 100 nm and one with a diameter of approximately 450 nm. These two populations could not be distinguished in the electron micrographs of the solutions of **6**. This type of bimodal distribution has also been reported for aggregates of so-called hyperextended amphiphiles.²⁴ Amphiphile **9** displayed a single type of spherical aggregate structure with a diameter of approximately 100 nm which agrees with the electron microscopy results (Figure 3B). Encapsulation experiments²⁵ were performed with the fluorescent dye ethidium bromide in order to determine whether the vesicles had a closed structure. A methanol solution containing amphiphile **6** was injected in water containing the positively charged dye and the resulting vesicle mixture was separated on a Sephadex column. The resulting gel permeation chromatogram (GPC) is shown in Figure 4. It indicates that the elution volume of the encapsulated dye is similar to that of the vesicles proving that closed vesicles are formed by **6**. The elution volume

(22) a) Koshland, D. E. Jr. *Prod. Natl. Acad. Sci. U.S.A.* **1958**, *44*, 98. (b) Jorgenson, W. L. *Science* **1991**, *254*, 954–955.

(23) Warner, M. *Colloid and Polymer Sci.* **1983**, *261*, 508–519.

(24) Menger, F. M.; Yamasaki, Y. *J. Am. Chem. Soc.* **1993**, *115*, 3840–3841.

(25) Fendler, J. H. *Membrane Mimetic Chemistry*; Wiley: New York, 1982.

(20) Rose, M. C.; Stuehr, J. *J. Am. Chem. Soc.* **1971**, *93*, 4350–4351.

(21) Nishio, M.; Hirota, M. *Tetrahedron* **1989**, *45*, 7201–7245.

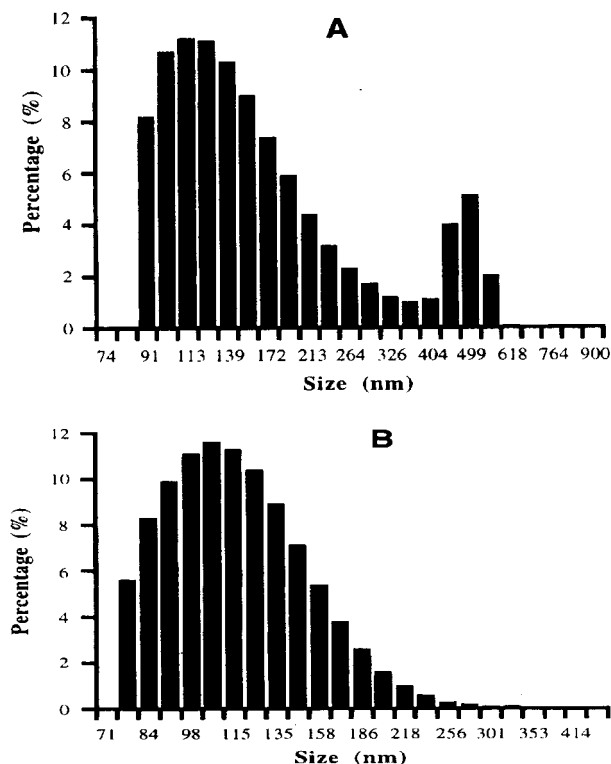


Figure 3. (A) Particle size distribution of **6** in water as determined by light scattering. (B) Particle size distribution of **9** in water as determined by light scattering.

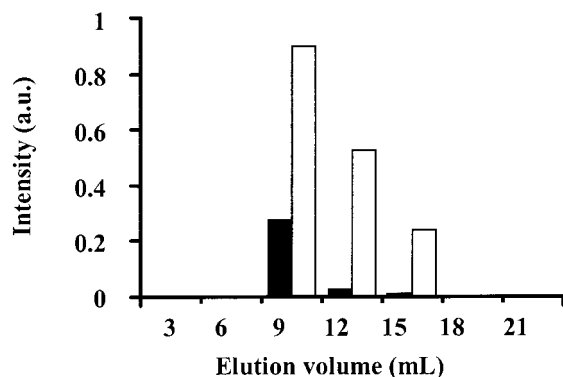


Figure 4. Gel permeation chromatogram showing the inclusion of ethidium bromide in vesicles formed by receptor amphiphile **6**. The black columns represent the intensity of the fluorescent dye and the white columns represent the absorbance of amphiphile **6**. The unencapsulated dye eluted as a broad band with an elution volume > 40 mL.

of the free dye was found to be much larger. X-ray diffraction was carried out on a cast film of a vesicle dispersion of amphiphile **6** dried on a silicon plate in vacuo. The diffraction patterns (Figure 5A) displayed a clear periodicity of 35 Å, which according to CPK space-filling models, indicates an intercalating bilayer arrangement of amphiphile **6**.

Monolayer experiments were performed with **4–6** in order to estimate the size of the headgroups of these amphiphiles (Figure 6). Molecular areas can be determined by extrapolating the slopes of the isotherms in the liquid condensed region. A molecular area of 190 Å² was obtained by extrapolation of the slope of the steepest part of the isotherm of amphiphilic compound **6**. The observed molecular areas for compounds **4** and **5** were found to be 220 and 180 Å², respectively. A value of 180 Å² corre-

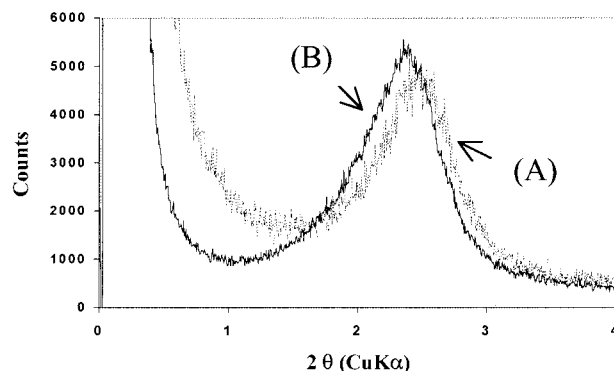


Figure 5. (A) X-ray powder diffraction on a film of a vesicle dispersion of **6** (A) cast on a silicon wafer and (B) that has been titrated with Magneson.

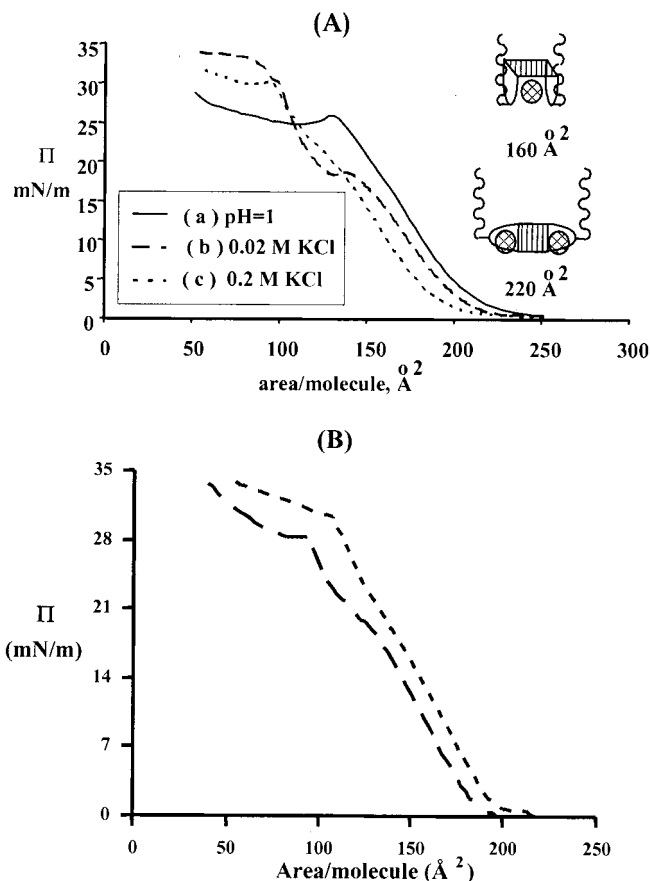


Figure 6. (A) Compression isotherms of compound **4** on different subphases: (a) pH = 1 and 6, (b) aqueous 0.02 M KCl, (c) aqueous 0.2 M KCl. On the right: schematic representation of the sandwich-like (top) and the stretched-out (bottom) conformations of the complex between **4** and K⁺. (B) Compression isotherms of compound **5** (—) and compound **6** (---) in deionized water. $T = 25$ °C.

sponds roughly to an area in which the receptor molecule has its crown ether parts fully extended (stretched out conformation). In the case of **4** the ester units presumably also contribute to the molecular area making it larger than the areas of **5** and **6**. Conductivity measurements can give information about the critical aggregate concentration (CAC) of our bowl-shaped surfactants.²⁶ This type of experiment was carried out with compounds **6** and **9**. For the former compound a value of 2.2×10^{-5} M

(26) Hessel, V.; Ringsdorf, H.; Laversanne, R.; Nallet, F. *Recl. Trav. Chim. Pays-Bas* **1993**, *112*, 339–346.

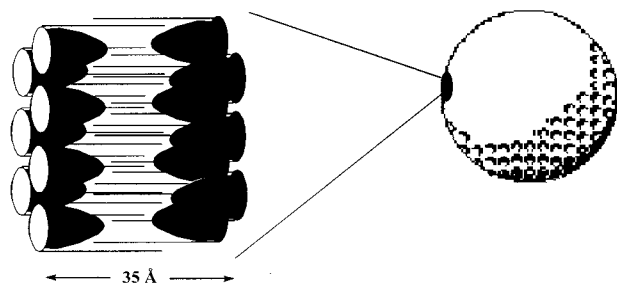


Figure 7. Schematic representation of the molecular golfballs formed by bowl-shaped amphiphile **6**.

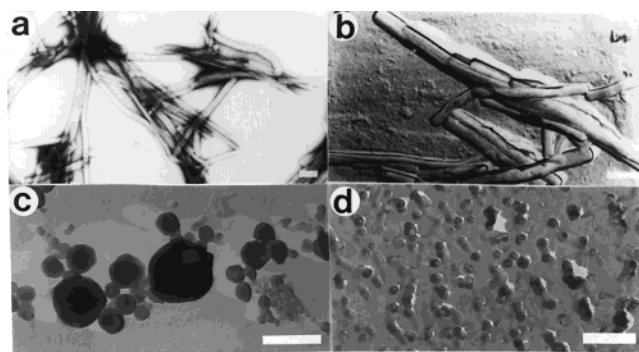


Figure 8. Transmission electron micrographs of dispersions in aqueous 0.1 N HCl of 0.2 wt % of amphiphile **4** ((a) negative staining, (b) freeze-fracturing) and amphiphile **5** ((c) Pt-shadowing). Bars represent 250 nm.

was found and for the later a value of 1.3×10^{-5} M. The CACs of amphiphiles **4**, **5**, and **8** could not be determined with this technique due to the low conductivity of these compounds in neutral water.

On the basis of the data presented above, we propose that the vesicles of amphiphilic receptor **6** and probably also of the other amphiphiles have the structure of a molecular golfball with dimples on its surface as is depicted in Figure 7. The thickness of the bilayer of **6**, as deduced from powder diffraction experiments, suggests that the hexadecylamine chains are intercalating.^{27,28} The crown ether moieties are facing the water phase in line with the monolayer experiments.

pH Dependent Aggregation Behavior. Dispersion of **4** in aqueous 0.1 N HCl afforded a white precipitate in a clear solution. Directly after sonication, EM revealed long tubelike structures with a diameter of 100 nm (Figure 8a,b). To prove that this material is not crystalline, we performed electron diffraction experiments: indeed no regular scattered patterns were observed. The freeze fracture electron micrographs (Figure 8b) showed that the tubes were built up from bilayered structures. Monolayer isotherms of **4** were found to be independent of the pH indicating that this molecule has the same conformation in both acidic and neutral water (molecular area of 220 Å², Figure 6a). When **4** was dispersed in aqueous solutions of intermediate acidity (viz., pH 5 and 3) EM revealed that directly after sonication only vesicles were present, whereas at lower pH values of 2 and 1.5 a mixture of vesicles and tube-like structures was visible. The relative ratio of tube-like structures to vesicle structures was proportional to the acidity of the solution (Figure 9). Even after 1 day, at pH = 3 a mixture of the

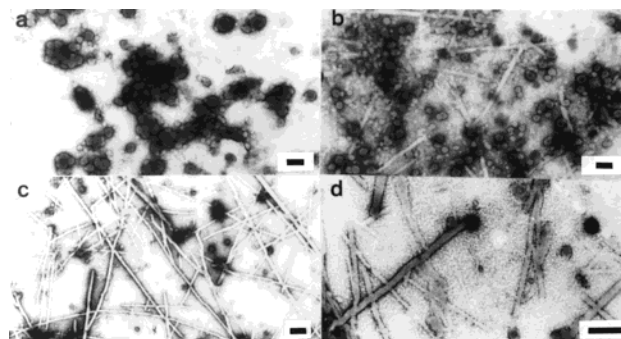


Figure 9. Transmission electron micrographs (negative staining technique) of dispersions of **4** (0.2 wt %) in solutions of different HCl concentration directly after sonication: (a) pH = 3, (b) pH = 2, (c) pH = 1.5, (d) pH = 1.5 (magnification). Bars represent 250 nm.

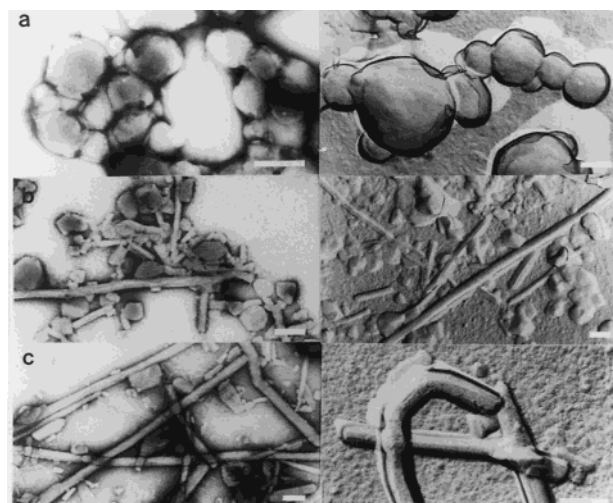


Figure 10. Transmission electron micrographs of dispersions of **4** (0.2 wt %) in (a) aqueous 0.2 M KCl, (b) aqueous 0.02 M RbCl, (c) aqueous 0.02 M CsCl. Bars represent 250 nm. Left: negative staining technique. Right: freeze fracturing technique.

two aggregates was found. Closer examination of the EM pictures of these mixtures provided insight into the origin of the tube-like aggregates: they were found to grow from "germinated" vesicles as can be seen in Figure 9d. Apparently, for this compound the tubelike structures are thermodynamically more stable than the vesicles in an environment of aqueous HCl. The rate of the tube formation is probably determined by the acidity of the solution. In contrast to **4**, when compound **5** was dispersed in aqueous 0.1 N HCl instead of in neutral water no significant changes in the structures of the aggregates were observed. In all cases, round vesicle structures of 25–300 nm were present even after some days (Figure 8c,d). Apparently, the ester functions in compound **4** play a role in the morphological change that is not observed for **5**.

Influence of Alkali Metal Ions on the Aggregation Behavior. Since bowl-shaped molecules derived from diphenylglycoluril are known to bind alkali metal ions,¹² we studied the aggregation behavior of **4** in aqueous 0.2 M KCl and NaCl solutions. Under these conditions, **4** was found to form large vesicles (diameters of 200–500 nm, Figure 10). Apparently, a change of the headgroup, from a protonated aza-crown ether ring to a ring containing an alkali metal ion, induces a change in the aggregation behavior. To investigate this effect in more detail, mono-

(27) Israelachvili, J. N.; Mitchell, D. J.; Ninham, B. W. *J. Chem. Soc., Faraday Trans. 2* **1976**, 72, 1525–1568.

(28) Kunitake, T. *Angew. Chem., Int. Ed. Engl.* **1992**, 31, 709–726.

layer experiments were performed using different subphases at 20 °C. The isotherms showed interesting differences between the acidic (and neutral) subphases and the subphases containing alkali metals (Figure 6A). The isotherms recorded on a subphase of 0.02 M NaCl and 0.02 M KCl solution were found to coincide. The isotherms in Figure 4A, curve b show the behavior of **4** on a 0.02 M KCl subphase. At a pressure of 19 mN/m a transition is observed, which disappears when the concentration of K⁺ ions in the subphase is increased to 0.2 M (Figure 6, curve c). From the onsets, extrapolating the slopes before and after the transition point, molecular areas of 220 and 160 Å², respectively, can be determined. These numbers suggest that at low pressures—and also at high K⁺ concentration—complex **4** has a relatively flat structure with two K⁺ ions bound in its crown ether rings. At high pressure the molecule adopts a sandwich-like conformation with only one K⁺ bound between the rings, in agreement with previous studies on clip molecules in solution.¹² This conformation is less likely for the protonated compound **4**·2H⁺ because of electrostatic repulsion. On a subphase of 0.002 M KCl the isotherm corresponded with the one recorded on pure water. We may, therefore, conclude that at this K⁺ concentration, there is no detectable complexation by **4**.

To study further the influence of the size of the alkali metal ion on the aggregation behavior of **4** we also used RbCl and CsCl in our experiments. Monolayer experiments showed that Rb⁺ and Cs⁺ ions are more strongly bound by **4** than K⁺ ions. Consequently, they could be studied at lower metal ion concentrations (0.02 M) at which also a significant phase transition was detected for each of these alkali metal ions. The molecular areas calculated for the different metal ions from the parts of the isotherms that correspond to the sandwich-like conformations are as follows: Na⁺, 155 Å²; K⁺, 160 Å²; Rb⁺, 165 Å²; Cs⁺, 180 Å². These areas were determined using the same concentration for all the metal ions, because, as it is known from the literature the position of the isotherms is dependent on the salt concentration.²⁹ The values mentioned above are in line with areas expected for sandwich complexes and it can be seen that they increase as the size of the metal ion increases. The headgroup becomes larger when a larger cation is complexed in the crown ether rings.

More detailed electron microscopy experiments revealed that in the presence of alkali metal ions both tubes and vesicles were formed and that the proportion of tubes relative to vesicles increased going from Na⁺ to K⁺ to Rb⁺, and then to Cs⁺. We propose that this variation is due to an increase in curvature of the aggregates when the size of the cation becomes larger, which is in line with the increase in molecular area measured in the monolayer experiments. Thus, addition of **4** (0.2 wt %) to a 0.02 M aqueous solution of RbCl gave vesicles and small rodlike aggregates (Figure 10b), whereas only tubelike structures were observed in the case of 0.02 M CsCl (Figure 10c). In contrast, the addition of **4** to a 0.2 M aqueous solution of RbCl or CsCl did not result in the formation of well-defined aggregates. Apparently, both the occurrence of a phase transition in the monolayer experiments and the type of aggregates formed in the aqueous dispersions depend on the concentration of the alkali metal ion.

Electron microscopy experiments on compound **5**, dispersed (0.2 wt %) in an aqueous 0.02 M solution of KCl, revealed the presence of large, round (multilayered) aggregates (200–1400 nm) as well as fields of smaller vesicles (80–100 nm) (Figure 11a,b). When larger metal ions (Rb⁺ and Cs⁺) were used in the experiments no major changes in the curvature of the aggregates were observed (Figure 11c,d) and round structures were mainly preserved. The difference in the aggregation behavior of **4** and **5** might be due to the presence of the ester functions attached to the crown ether moieties in the former compounds, which can participate in the metal ion coordination. In that case, a change in the size of the alkali metal ion would have an important effect on the headgroup of amphiphile **4**, and in turn on the curvature of the aggregates, but not on the headgroup of **5**.

Complexation of Magneson in Water. Host–neutral guest binding studies were performed on the vesicle forming receptor molecules **6**, **8**, and **9** in water. Magneson was used as the guest, and the titration experiments were followed by UV–vis spectroscopy. The titration curves of amphiphile **9** under and above the CAC are shown in Figure 12A and B.³⁰ The same type of binding curves were obtained for amphiphile **6**. When Magneson was added to the two bowl-shaped hosts no change in the type of aggregates was observed by electron microscopy. In water, below the CAC of **6** and **9**, Magneson is bound in a 1:1 host–guest ratio, as can be concluded from the titration curves. The association constants calculated from these curves are $K_a = 1 \times 10^6$ M⁻¹ and $K_a = 15 \times 10^6$ M⁻¹ for hosts **6** and **9**, respectively.³¹ These values are very high when compared to those in chloroform ($K_a < 5000$ M⁻¹). They are of the same order of magnitude as those found for amphiphilic cyclophanes with nonionic guests.⁹ The titration curves of **6** and **9** with Magneson above the CAC of the amphiphile could only be fitted if it was assumed that only half of the host molecules are involved in the binding process. In that case, a good correlation for a 2:1 host–guest ratio was obtained with a binding constant $K_a = 4 \times 10^5$ M⁻¹ in the case of **6** and a binding constant $K_a = 7 \times 10^5$ M⁻¹ in the case of **9**. These results suggest that only the dimples at the outer face of the “golfballs” are accessible to guest molecules and that the inner part of the aggregates cannot be reached. X-ray diffraction performed on a cast film of a vesicle dispersion of amphiphile **6** which had been titrated with the guest displayed a clear periodicity of 38 Å (Figure 5B). Inspection of CPK models showed that this periodicity may correspond to intercalated bilayers (35 Å) which have at one side molecules of Magneson complexed to molecules of **6**.³²

Figure 12C shows the titration curve for the vesicles of amphiphile **8** with Magneson above the CAC. This curve reveals that above this concentration Magneson is bound in a 1:1 host–guest ratio with a binding constant

(30) In water, NMR measurements could not be used for this purpose because of the occurrence of broad signals due to aggregation of the amphiphilic receptor molecules. Only the tosylate counterions gave sharp signals which indicates that the anions are only partly associated with the aggregates in the water phase.

(31) The K_a 's are approximate since the measurements could not be carried out at the optimum concentrations of host and guest required for the titration experiments. If a lower host concentration was used the absorbance of the guest became too low to be measured. For a discussion of the determination of binding constants see: Weber, G. In *Molecular Biophysics*; Pullman, B., Weisbluth, M., Eds.; Academic Press: New York, 1965; p 369.

(29) Aston, M. S. *The structural dynamics and equilibrium properties of colloidal systems*; Bloor, D. M., Wyn-Jones, E., Eds.; Kluwer Academic Publisher: Amsterdam, 1990; p 551.

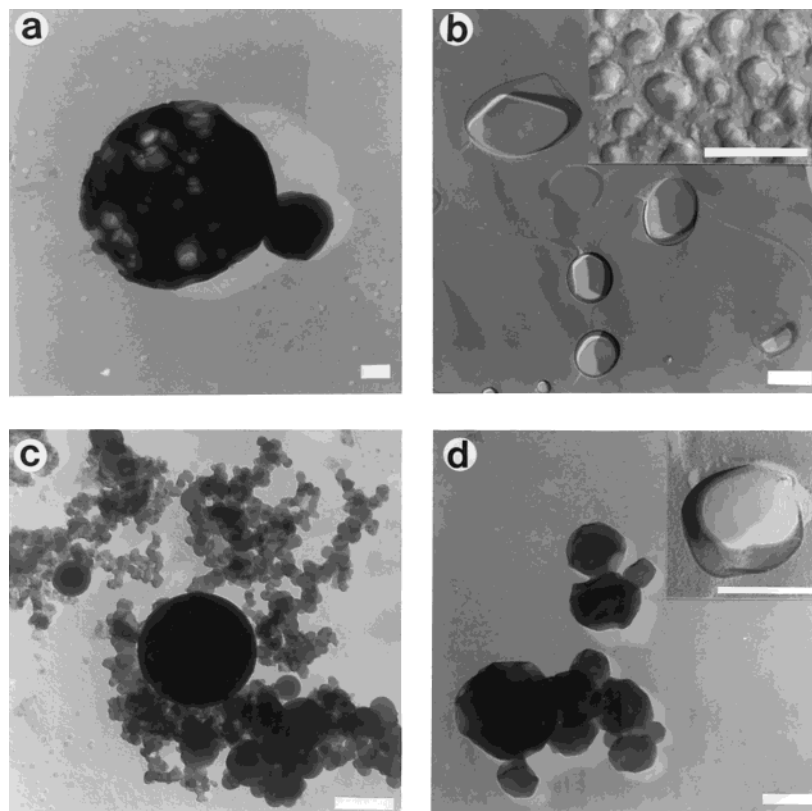


Figure 11. Transmission electron micrographs of dispersions of **5** in (a) 0.02 M KCl (Pt-shadowing), (b) 0.02 M KCl (freeze fracturing), (c) 0.02 M RbCl (Pt-shadowing), and (d) 0.02 M CsCl (freeze fracturing). Bars represent 200 nm.

of $K_a = 4 \times 10^5 \text{ M}^{-1}$. This measured host–guest ratio is in contrast to the ratios measured for **6** and **9** and indicates that the binding sites of all the host molecules of **8** are accessible to the guests.

Electron microscopy experiments revealed that when Magneson is bound by host molecule **8** adhesion of the vesicles into linear aggregates occurred. In some cases the linear aggregates further developed into tube-like structures (Figure 13a,b). With resorcinol as a guest, assemblies of adhered vesicles were also observed, but tube-like structures were not found (Figure 13c). Recently, it has been proposed that vesicle adhesion is the result of van der Waals interactions between the headgroups coupled to bilayer flexibility.³³ In our case, the binding of the guest could increase these attractive van der Waals interactions between the headgroups, viz. by changing their polarity leading to extended structures. The size of the guest can also have an important effect on the curvature of the aggregates. Hence, a change in both size and polarity of the headgroup can explain the observed behavior. We know from NMR experiments in CDCl_3 that amphiphile **8** can exist in three conformations and that the binding of the guest occurs via an induced fit mechanism (vide supra). This mechanism may also play a role in the change of the aggregate structure although it is remarkable that such a change was not observed for amphiphiles **6** and **9**. The fact that contrary

to **6** and **9** a 1:1 host–guest ratio is found for **8** above the CAC can be explained by the morphological changes from vesicles to tubules which apparently makes the cavities on the inside of the vesicle available for guest binding.

Conclusions

We have shown that aggregates displaying high binding affinities toward guest molecules can be formed from amphiphilic bowl-shaped molecules derived from diphenylglycoluril. These aggregates can have different structures, i.e. vesicles or tubules, which in the case of the ester containing receptor **4** can be tuned by adding different alkali metal ions. Monolayer experiments show that this behavior is presumably coupled to a conformational change in this amphiphilic receptor. In water, molecules of **4** have a stretched-out conformation which changes to a sandwich-like conformation upon binding of alkali metal ions. Increasing the size of the alkali metal ion from Na^+ or K^+ to Rb^+ and then to Cs^+ , leads to an increase in curvature of the aggregates and hence to a gradual change in their shape, viz. from vesicles to tubules. Binding studies on vesicles of **6** and **9** with Magneson revealed that below the CAC of the amphiphile 1:1 host–guest complexes are formed. Above the CAC only half of the binding sites are accessible for these guest molecules, suggesting that only the cavities on the outer side of the vesicles can be occupied. In one case (amphiphile **8**), the binding of the guest causes the vesicles to adhere and even to change into tubular structures. Thus, we have shown an example of how supramolecular structures can be tuned by the addition of metal ions and organic guest molecules in a similar way as natural cell membranes.

(32) Note: We have more confidence in the present result for the bilayer thickness (35 Å) than in the result reported earlier (53 Å, ref 13) for the following reasons: (i) The present result is based on a diffractogram that was taken at low angle (Figure 5) and unambiguously shows the presence of the first-order reflection at a 2θ value corresponding to a periodicity of 35 Å and absence of one corresponding to 53 Å; (ii) The present result of an interdigitated bilayer gives a better match of the cross sections of alkyl tails and headgroups (Figure 7).

(33) Petsev, D. N. *Langmuir* **1999**, *15*, 1096–1100.

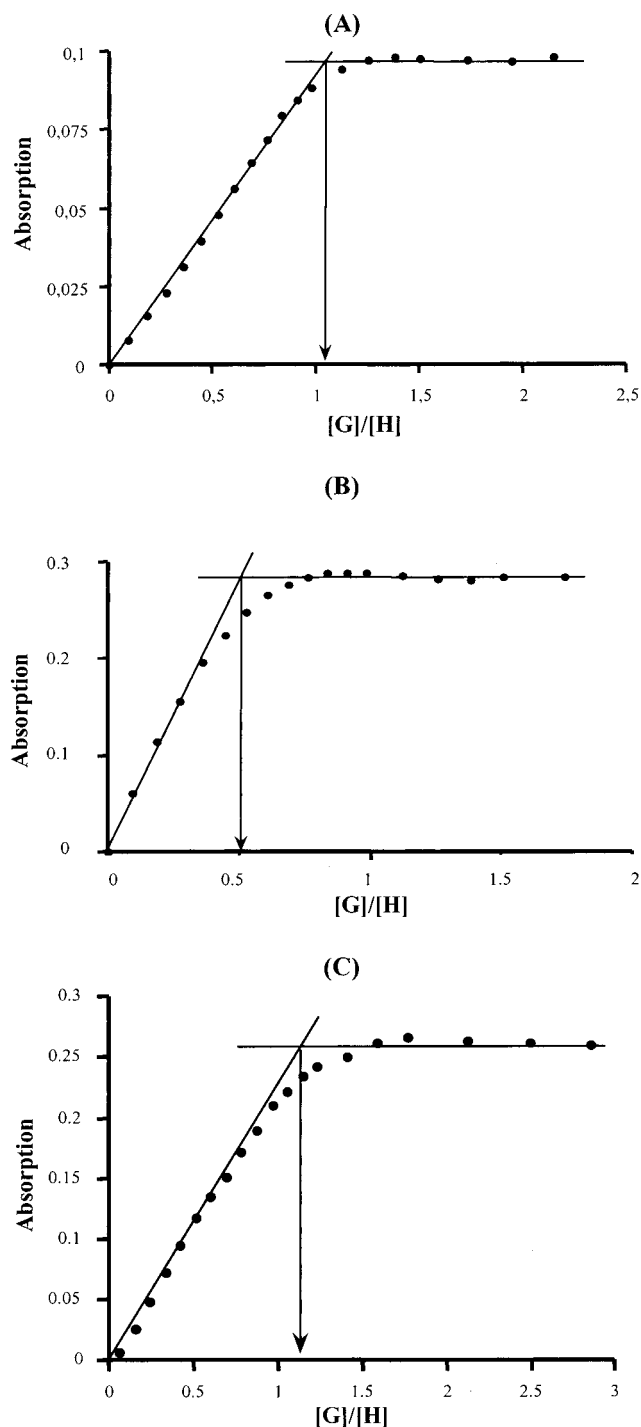


Figure 12. Titration curve of Magneson (G) with bowl-shaped amphiphile **9** (H) (A) under the CAC in water at $T = 25\text{ }^{\circ}\text{C}$, $[\text{H}] = 9.0 \times 10^{-6}\text{ M}$ and (B) above the CAC of **9**, $T = 25\text{ }^{\circ}\text{C}$, $[\text{H}] = 2.0 \times 10^{-4}\text{ M}$. (C) Titration of Magneson with **8** above the CAC in water, $[\text{H}] = 2.0 \times 10^{-4}\text{ M}$.

Possible applications of the above-described structures can be foreseen in the fields of sensory systems, drug delivery, and chromatographic separation of organic molecules.

Experimental Section

General Methods. CH_2Cl_2 and CHCl_3 were distilled from CaH_2 , and THF was distilled from LiAlH_4 . The syntheses of the compounds **1**, **2**, and **7** have been previously reported.^{11a}

Receptor Compound 3. This compound was prepared according to a procedure developed in our laboratory^{11a} using

compound **2** (3.0 g, 3.0 mmol), 3-aminopropanol (228 mg, 3.0 mmol), Na_2CO_3 (10.1 g, 0.11 mol), and NaI (30.3 g) in 400 mL of acetonitrile. The amino alcohol was added during a period of 2 days to the refluxing mixture of the other components and then reflux was continued for 1 week. The product was purified by flash column chromatography (eluent $\text{CHCl}_3/\text{MeOH}/\text{triethylamine}$, 96/3/1, v/v/v) and subsequent precipitation in hexane to afford **3** as a white powder in 70% yield: mp $> 250\text{ }^{\circ}\text{C}$ dec; ^1H NMR (90 MHz, CDCl_3) δ 7.09 (s, 10H), 6.69 (s, 4H), 5.60 and 3.69 (2d, 4H, $J = 16\text{ Hz}$), 4.35–3.65 (m, 28H), 2.94 (t, 12H), 1.74 (t, 4H); FAB-MS (*m*-nitrobenzyl alcohol, m/z) 993 ($\text{M} + \text{H}$)⁺. Anal. Calcd for $(\text{C}_{54}\text{H}_{68}\text{N}_6\text{O}_{12} \cdot \text{HCl})$: C, 62.99; H, 6.75; N, 8.16. Found: C, 62.81; H, 6.70; N, 8.11.

Receptor Compound 4. Compound **3** (1 mmol) was suspended in dry CH_2Cl_2 (20 mL) and triethylamine (20 mL) under an argon atmosphere. Decanoyl chloride (4 mmol) was added, and the reaction mixture was stirred at room temperature (48 h). The reaction mixture was diluted with CH_2Cl_2 (40 mL) and washed with aqueous 1 N HCl (2 \times), saturated aqueous NaHCO_3 (2 \times), and water. The organic layer was dried (MgSO_4), and the solvent was vacuum evaporated. The crude product was purified in two steps, first by flash column chromatography (eluent 0.5 vol % MeOH, 1 vol % Et_3N in CHCl_3) and subsequently by dissolving it in CHCl_3 and washing the resulting solution with 1 N aqueous HCl (2 \times) and a saturated aqueous NaHCO_3 solution (2 \times). The organic layer was dried (MgSO_4) and evaporated to dryness to yield the pure compound. The product was obtained in 75% yield: mp $148\text{ }^{\circ}\text{C}$ dec; ^1H NMR (90 MHz, CDCl_3) δ 7.07 (s, 10H), 6.69 (s, 4H), 5.62 (d, 4H, $J = 16\text{ Hz}$), 4.3–3.5 (m, 32H), 2.88 (t, 8H), 2.69 (t, 4H), 2.28 (t, 4H), 2.0–1.1 (m, 40H), 0.79 (t, 6H); FAB-MS (m/z) 1357 ($\text{M} + 1$)⁺. Anal. Calcd for $(\text{C}_{78}\text{H}_{112}\text{N}_6\text{O}_{14})$: C, 69.00; H, 8.31; N, 6.19. Found: C, 68.67; H, 8.44; N, 6.27.

Receptor Compound 5. This compound was prepared as described for **3** using 2 g (2 mmol) of compound **2**, 20 g (133 mmol) of NaI, 6.5 g (61 mmol) of Na_2CO_3 , and 1.2 g (4.98 mmol) of 1-hexadecylamine in 500 mL of acetonitrile. The solvent was evaporated, 200 mL of aqueous 0.5 M NaOH was added, and the resulting suspension was extracted with CHCl_3 (3 \times). The organic layer was washed with aqueous 0.5 M NaOH, dried (MgSO_4), and evaporated to dryness. After column chromatography (eluent $\text{CHCl}_3/\text{MeOH}/\text{triethylamine}$, 94/5/5, v/v/v), 1.93 g (73%) of **5** was obtained as a white powder: mp $187\text{ }^{\circ}\text{C}$; ^1H NMR (90 MHz, CDCl_3) δ 0.80 (t, 6H), 1.19 (s, 52H), 1.80 (m, 4H), 2.52 (t, 4H), 2.80 (t, 8H), 4.3–3.4 (m, 28H), 5.57 (AX pattern, 4H), 6.72 (s, 4H), 7.10 (s, 10H); FAB MS $m/z = 1326$ ($\text{M} + \text{H}$)⁺. Anal. Calcd for $\text{C}_{80}\text{H}_{120}\text{N}_6\text{O}_{10} \cdot \text{H}_2\text{O}$: C, 71.50; H, 9.15; N, 6.25. Found: C, 71.86; H, 9.13; N, 6.24.

Receptor Compound 6. A mixture of 0.3 g (0.23 mmol) of compound **5** and 0.5 g (2.7 mmol) of methyl tosylate in 50 mL of toluene was refluxed under nitrogen for 1 week. The solvent was evaporated, and the solid was washed with diethyl ether to remove the excess of methyl tosylate. Compound **6** (0.28 g, 90%) was obtained as a yellow/white powder: mp $210\text{ }^{\circ}\text{C}$; ^1H NMR (90 MHz, CDCl_3) δ 0.86 (t, 6H), 1.24 (s, 52H), 1.80 (m, 4H), 2.30 (s, 6H), 4.6–3.2 (m, 42H), 5.61 (d, 4H), 6.58 (s, 4H), 7.13 (m, 14H), 7.81 (d, 4H); FAB MS m/z 1525 ($\text{M} - \text{Tos}$), 1339 ($\text{M} - \text{Me} - 2\text{Tos}$). Anal. Calcd for $\text{C}_{96}\text{H}_{140}\text{N}_6\text{O}_{16}\text{S}_2 \cdot 3\text{H}_2\text{O}$: C, 65.80; H, 8.40; N, 4.80; S, 3.66; Found: C, 65.67; H, 8.11; N, 4.84; S, 3.88.

Receptor Compound 8. This compound was prepared as described for **3** using 1.17 g (1.1 mmol) of **7**, 12 g (80 mmol) of NaI, 3.8 g (35.6 mmol) of Na_2CO_3 , and 0.81 g (3.36 mmol) of 1-hexadecylamine in 400 mL of acetonitrile. The solvent was evaporated, 200 mL of aqueous 0.5 M NaOH was added, and the resulting suspension was extracted with CHCl_3 (3 \times). The organic layer was washed with aqueous 0.5 M NaOH, dried with MgSO_4 , and evaporated to dryness. After column chromatography (eluent $\text{CHCl}_3/\text{MeOH}/\text{triethylamine}$, 98/1/1, v/v/v), 0.94 g (60%) of **8** was obtained as a white powder: mp $128\text{ }^{\circ}\text{C}$; ^1H NMR (200 MHz, CDCl_3) δ 0.87 (t, 6H), 1.25 (m, broad, 52H), 2.70 (m, 4H), 3.0 (m, 8H), 4.35–3.5 (m, 20H), 4.60 (m, 4H), 4.8 (d, $J = 14.5\text{ Hz}$, 2H, *sa* conformation), 5.1 (d, $J = 16\text{ Hz}$, 4H, *ss* conformation), 7.8–6.0 (m, 18H, see Table 1 for details); FAB MS $m/z = 1426$ ($\text{M} + \text{H}$)⁺. Anal. Calcd for

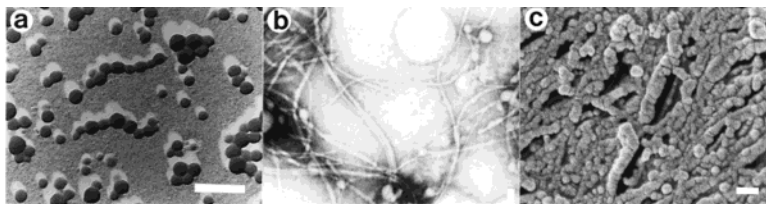


Figure 13. (a, b) Transmission electron micrographs of dispersions of amphiphile **8** in water to which 1 equiv of Magneson has been added. (a) Pt-shadowing, (b) negative staining. (c) Scanning electron micrograph of **8** in water to which 1 equiv of resorcinol has been added (freeze-fracturing). Bars represent 200 nm.

$C_{88}H_{124}N_6O_{10} \cdot H_2O$: C, 73.20; H, 8.80; N, 5.82. Found: C, 73.23; H, 8.80; N, 5.71.

Receptor Compound 9. This compound was prepared as described for **6** using 0.38 g (0.27 mmol) of compound **8** and 1 g (5.4 mmol) of methyl tosylate. Compound **9** (0.35 g, 89%) was obtained as a yellowish powder: mp 113 °C; 1H NMR (400 MHz, CD_3OD , see Table 1 for details) δ 0.85 (t, 6H), 1.4–1.22 (m, 52H), 1.9 (m, 4H), 2.32 (s, 6H), 4.5–3.2 (m), 4.1 (m, 2H, *sa* conformation), 4.8 (d, J = 14 Hz, 4H, *sa* conformation), 5.1 (d, J = 15 Hz, 4H, *ss* conformation), 5.8 (d, J = 16 Hz, 4H, *aa* conformation), 6.1 (m, 2H, *sa* conformation), 7.8–6.2 (m, 26H); FAB MS m/z 1627 ($M - Tos$), 1456 ($M - 2Tos$). Anal. Calcd for $C_{104}H_{144}N_6O_{16}S_2 \cdot H_2O$: C, 68.77; H, 8.10; N, 4.63; S, 3.53. Found: C, 68.67; H, 7.90; N, 4.60; S, 3.64.

Magneson (10). This molecule was purchased from Sigma (90% pure) and purified by column chromatography (eluent $CHCl_3/MeOH/triethylamine$, 89/10/1, v/v/v) followed by recrystallization from methanol: mp 199 °C; 1H NMR (400 MHz, CD_3OD , 25 °C) δ 6.30 (d, 1H, J = 2.5 Hz), 6.55 (q, 1H, J = 9.0 Hz, J = 2.5 Hz), 7.83 (d, 1H, J = 9.0 Hz), 7.95 (AX pattern, 2H), 8.36 (AX pattern, 2H); UV–vis ($CHCl_3$) λ_{nm} 392; UV–vis (H_2O (pH = 10)) λ_{nm} 556.

Preparation of the Aggregates. The desired amount of the different amphiphiles was dissolved in 100 μL of ethanol/THF (1/2, v/v). An amount of 50 μL of this solution was injected into 5 mL of deionized water or the required aqueous solution at 25 °C, while vortexing. Amphiphile **4** was dissolved in 1 drop of $CHCl_3$ and dispersed into the appropriate aqueous solution. The dispersion was heated and sonicated at 70 °C for 30 min. Samples for EM studies were taken at different times, between 1 h and 2 weeks.

Electron Microscopy. Negative Staining Technique. A droplet of a sample was placed on a Formvar coated copper grid. After allowing adsorption on the grids for 2 min, the solution was drained with filter paper and the samples were stained with an aqueous uranyl acetate solution (1 wt %) which was removed after 1 min. **Freeze-Fracturing Technique.** Samples were prepared by bringing a drop of the dispersion onto a golden grid, placed between two copper plates, and fixated in supercooled liquid nitrogen. The sample was placed in a Balzers Freeze Etching System BAF 400 D at 10^{-7} Torr and heated to -105 °C. After fracturing, the sample was etched for 1 min (ΔT = 20 °C), shadowed with Pt (layer thickness 2 nm), and covered with carbon (layer thickness 20 nm). Replicas were allowed to heat up to room temperature and left on 70% aqueous sulfuric acid for 24 h. After rinsing with water they were allowed to dry and studied using a Philips TEM microscope. For SEM measurements the freeze-fractured sample was shadowed with Au and studied using a JEOL JSM-6330F field emission gun scanning electron microscope. **Pt-Shadowing Technique.** Samples were prepared by bringing a drop of the dispersion onto a Formvar coated microscope grid. After 1 min, the excess of dispersion was drained and the sample was shadowed by evaporation of Pt under an angle of 45°.

Conductivity Measurements. Conductivity measurements were performed with a Schott Geräte CG 852 Konduktometer with a platinum electrode at room temperature. A stock solution of 30 mL was diluted 10 times with 1 mL of water and the conductivity was continuously monitored. Then 10 mL of the diluted solution was removed and the same procedure was repeated until very dilute concentrations were achieved.

Encapsulation Experiments. The encapsulation of ethidium bromide was measured by gel permeation chromatography (GPC) in combination with fluorescence and UV–vis spectroscopy. Vesicle solutions in water containing 1×10^{-4} M ethidium bromide were prepared as described above. The dispersions were passed over a Sephadex G50 column with water as the eluent. The fractions were collected and the fluorescence intensity of ethidium bromide (λ_{ex} = 480 nm, λ_{em} = 620 nm), as well as the absorbance of the amphiphile at λ = 300 nm were measured to calculate the dye and amphiphile concentrations.

X-ray Powder Diffraction. Samples were prepared by placing a drop of a vesicle suspension on a silicon single-crystal sample holder and the system was evacuated to 0.1 Torr. Powder diffraction measurements were carried out on a commercial Philips X-ray powder diffractometer or on a home-built (NIOZ, Texel) Bragg–Brentano diffractometer, optimized for low-angle measurements.³⁴ The X-ray tube was ceramic with a long fine focus and gave Cu–K α radiation (generator 40 kV, 40 mA). The goniometer had a variable divergence and variable anti-scatter slits. The detector, with the receiver slit at 0.1 mm, was of the Peltier-cooled Si/Li type. The instrument was mounted in a chamber of which the relative humidity could be controlled by a humidifying instrument flushed with He gas.

Particle Size Distributions. Particle size distributions of our vesicle dispersions were determined at 25 °C by dynamic light scattering using a Malvern Autosizer IIc apparatus at an angle of 90°. Vesicle samples were prepared as described above.

Monolayer Experiments. Surface–pressure surface area diagrams (Π/A isotherms) were recorded on a home-built thermostated trough (195 cm²) equipped with a Wilhelmy balance. In a typical experiment, 25 μg of amphiphile in 50 μL of $CHCl_3$ was spread on the subphase (T = 20 °C), and after 15 min the monolayer was compressed at a rate of 7.0 cm²/min.

Binding Studies. Association constants in chloroform were determined by 1H NMR following the shift of appropriate host and guest protons and by UV–vis following the absorption of the guest Magneson at 438 nm as a function of the guest concentration (0 – 2×10^{-4} M). For both types of experiments the same constant host concentration was used (5×10^{-4} M). In water under the CAC of **5** and **9** the absorbance of Magneson was monitored at 450 nm as a function of the guest concentration (0 – 1.8×10^{-5} M) with a constant host concentration of 9.0×10^{-6} M. Above the CAC of **5** and **9**, the absorbance of Magneson was monitored at 534 nm as a function of the guest concentration (0 – 5.0×10^{-4} M), with a constant host concentration of 2.0×10^{-4} M. In the case of host **8**, the absorbance of Magneson was monitored at 450 nm. The titration curves were obtained by subtracting the absorption of the free guest from the measured absorption. The errors in the binding constants are approximately 10% and 50% for the experiments in chloroform and water, respectively.

Acknowledgment. B.E thanks E.C. for a postdoctoral Marie Curie TMR grant.

JO000770T

(34) Kühnel, R. A.; van der Gaast, S. J. In *Advances in X-ray analysis*, Vol 36; Gilfrich, J., et al., Eds.; Plenum Press: New York, 1993.